SCA-9818

DESATURATING SHALEY SANDS: PHYSICAL AND RESISTIVITY MODELING

E. M. Withjack*, Western Atlas, J. R. Durham, Spirit Energy,
A. Kh. Mirzajanzade, T. Cheidaev, S. Saruyev and
A. Suleimanov, Azerbaijan State Oil Academy

ABSTRACT

This paper describes laboratory and theoretical studies of capillary displacement and resistivity modeling for thinly-bedded, shaley sands. Core material is taken from a well-characterized formation in the Gulf Coast region (Yegua, Orange Co., Texas), and is used here as an analog for reservoirs in the South Caspian basin (Azerbaijan). The laboratory program makes simultaneous saturation (x-ray computed tomography) and electrical resistivity measurements during low-rate, capillary displacement of brine by oil. A theoretical model is presented for representing capillary displacement as a sequence of events dominated by different mechanisms. Localized saturation measurements within the core are incorporated in a mathematical resistivity model that explicitly determines saturations in the sandstone (hydrocarbon bearing) regions.

INTRODUCTION

This paper presents the results of capillary displacement tests and resistivity modeling for thinly-bedded, shaley sandstone rock. Saturation and electrical resistivities are measured simultaneously using x-ray computed tomography (CT).[1] Core material, taken from a well-characterized formation in the Gulf Coast region, was selected as an analog for several reservoirs in the South Caspian basin (Azerbaijan).[2,3,4] A mathematical resistivity model is described that incorporates local CT saturation measurements and determines saturations within the sandstone regions of a core. The model is based on a variation of parallel-conductor theory.[5-8] A theoretical model is also described for representing capillary displacement as a sequence of events dominated by different mechanisms.[9] Results from the capillary model successfully represent displacement behavior, while the resistivity model provides good agreement with experimentally determined saturations.

EXPERIMENTAL PROGRAM

The primary objective of the experimental program was to determine local saturations in a core sample undergoing resistivity testing to provide key information for the mathematical modeling.

* Previously with Unocal Corp.

Sample Selection and Preparation. The selected core material was taken from a Gulf Coast well (Rita Gonzales #1) in the Yegua formation, Orange Co., Texas. The core consisted of interbedded, very fine-grained sandstones and laminated-to-burrowed, silty claystones and siltstones. Two core plugs (**Table 1**) were cut: 13,116.7 ft (Sample #1) and 13,140.8 ft (Sample #2). Both plugs are thinly laminated with shales (**Fig. 1**), although Sample #1 has a more massive streak located in the upper portion of the core. X-ray diffraction data from the two plugs indicate bulk clay mineralogy as: detrital kaolin, avg. 16 wt % (range = 14 to 17 wt %), illite; avg. 18 wt % (range = 8 to 27 wt %), and minor amounts of chlorite; avg. 3 % (range = 2 to 3 wt %). Clays are concentrated within the laminations and also appear as grain coating material.

The extracted plugs were initially flushed with a synthetic brine to remove dissolved salts and drilling contaminants. The samples were then flushed sequentially with toluene and methanol in preparation for final brine saturation.

Test Fluids. The test brine (undoped fluid) was composed mainly of sodium chloride and calcium chloride. The resistivity was of 0.44 ohm-m, while specific gravity and viscosity were 1.005 gm/cc and 1.00 cp, respectively. The oil (MO) was a mixture of a heavy solvent and dodecane, mixed with iododecane, with a resulting viscosity of 2.5 cp and a specific gravity of 0.85 at 21°C.

Test Apparatus and Procedure. The CT scanner was a modified medical head scanner. The core was mounted within a rubber sleeve under confining pressure in an aluminum core holder. The outlet end of the core was in capillary contact with a water-permeable ceramic disk. Electrical connections (2-electrode method) were provided at both ends of the core. Injection pressures were held by computerized pump. The in-situ saturations of oil and water were determined directly from the x-ray CT data, although checked volumetrically by pipette. Nine equally-spaced CT slices (1.5 mm) were taken along the length of the core. Each experiment took several months, as each level of capillary pressure typically required a stabilization time of 3 to 7 days. The criteria for capillary equilibrium were stability of both electrical resistance and saturation.

EXPERIMENTAL RESULTS

The results of the displacement test for Sample #1 are shown in **Fig. 2**. The direction of oil injection is from left to right. Note that the orientation (top) of the CT scans approximately correspond with the core photos. The cross-sectional slices for each row show the steady-state conditions at a particular level of capillary pressure. The brighter grays correspond to higher oil saturations, except where there are some high-density locations at the top of the core which appear bright at all capillary pressures. The water initially present in the lower (sandstone) part of the core was readily displaced by oil. The shale streaks appear to remain dark and absorb little oil, although close inspection on a higher-resolution monitor indicated that water was displaced from some thin sand stringers between the shale laminations.
Fig. 3 shows the CT slices corresponding to the different capillary pressures for Sample #2. At 15 psi (**Fig. 3b**), the oil distribution shows a "shielding" effect caused by the curved shale band in the upper part of the core. This effect results in a delay in the displacement of brine from the sandy region above the shale; apparently, oil flows around the shale band to displace brine from upper regions in the downstream part of the core. The presence of many, thin shale stringers contributes to the banded displacement pattern in the downstream half of the core.

Average water saturations along the length of Sample #1 are plotted in **Fig. 4**. With the exception of the 5 psi displacement, these tests resulted in slightly decreasing water saturations along the first half of the core, and slightly increasing water saturations in the downstream half (particularly for pressures > 60 psi). This reflects the fluid distributions in **Fig. 2**, which show larger cross-sectional areas displaced by oil for slices near the mid section of the core. **Fig. 5** shows the brine profiles for Sample #2. The influence of

the curved shale band appears to dominate the displacement in the upsteam half of the core. At the highest capillary pressure (150 psi), the saturation gradient persisted even after 5 days of desaturation.

Capillary Pressures. **Fig. 6** shows the capillary pressure curves determined from the oil-brine displacements and those from mercury-injection tests. These data are in reasonable agreement, considering that the latter are based on estimated interfacial tensions and contact angles. The pore-throat size distributions calculated from the mercury injection data indicated a bimodal distribution with peaks at about 5 microns and 0.01 microns.

Resistivity Measurements. **Table 2** summarizes the results of the resistivity measurements. The table lists the capillary pressures, water saturations (average and local sandstone), resistance, resistivity and resistivity index for each core. A plot of resistivity index versus water saturation (**Fig. 7**) is characteristic of low-resistivity core. As indicated by others, a log-log plot of resistivity index versus water saturation can result in nonlinearities that are not possible to interpret in terms of the simple Archie equation.[6] This behavior has led to the formulation of several alternative mathematical models using electrical conductance analogs.[5-8]

CAPILLARY BEHAVIOR MODELING

The mechanism of the desaturation process was investigated by theoretical modeling. Generally, an evolutionary process may be modeled using a set of exponential functions of the form (hereafter referred to as EM technique):

$$Y_i(t)=A_i-B_i \exp(-\alpha_i t) \qquad (1)$$

where, Y_i is water expelled over a particular segment of a desaturation process; A_i, B_i and α_i are the associated growth constants. Modeling the complete behavior of a desaturation process requires a summation of functions to represent the process. The functions are selected to best represent the data, but are without regard to the mechanistic displacement processes.

The transition from one displacement regime to another may, in concept, be caused by the beginning of new activity and the termination of the influence of a previous activity. A more appropriate approach may be expressed by the following:[9]

$$Y=\Sigma A_i[1- \exp(\alpha_i t)] \qquad (2)$$

where the summation is over *n* exponential functions. Note that each A_i is the limit for a particular desaturation term, and therefore the total limit of the desaturation is equal to the sum of A_i. Eq. 2 is referred to as Tobolsky's Technique (TT) in the Former Soviet Union.

Capillary Modeling Procedure. For the EM procedure (Eq. 1), based on some number (k) of initial experimental points, the best parameters and standard deviations were calculated. Then the next point (k+1) was included and the standard deviation recalculated. If its value increased, the beginning of a new stage was considered to be established and a new exponential model was constructed. Otherwise, the first exponential term was considered still valid and the next (k+2) point was tested.

According to the TT approach, the parameters for Eq. 2 can be determined by separating existing exponents one-by-one, starting from the end of a given data set. For this approach, the total limit A_∞ must be determined beforehand by use of a forecasting technique. Here, EM was used to obtain A_∞. Next, the difference (A_∞ -Y) for all t is calculated. This may be expressed as:

$$A_\infty - Y = \Sigma A_i \exp(-\alpha_i t), \quad (3)$$

Mechanistic insight may be obtained from a plot of $\ln(A_\infty - Y)$ versus time t. If the last points for some duration of time may be approximated by a straight line, then only one exponent was active during that period. The parameters A_n and α_n can be determined from the plot as $\ln A_n$ = Intercept, and α_n= Slope. The beginning of the current activity corresponds to the termination of the influence of the previously acting exponent. The exponential term $A_n\exp(-\alpha_n t)$ is excluded from further consideration by subtracting it from the data set, and a new plot is constructed in $\ln[(A_\infty - Y - A_n\exp(-\alpha_i t)]$ versus t coordinates. Parameters of the next exponent A_{n-1} and α_{n-1} are then determined from the plot and the procedure is continued.

Capillary Modeling Results. **Tables 3** and **4** summarize the modeling results for the capillary displacement tests as calculated by EM and TT, respectively. The tables list the time steps and duration for each of the acting exponential functions, and parameters A_i, B_i and α_i. The numbers in parenthesis (**Table 3**, Time Step) indicate the actual end time of a particular capillary pressure. The last column provides a projection of the time required to reach the theoretical 99.99% completion of the process.

For the Berea displacement, the TT model subdivides the saturation processes into three exponential functions. The resulting equation, for example, was determined as:

$$Y = 0.219[1-\exp(-0.20288t)] + 12.58[1-\exp(-0.00479t)] + 1.304[1-\exp(-0.00161t)]$$

Figs. 8a through **8c** illustrate the determination of the terms; **Fig. 8d** shows the influence of the constituent exponents and results of the final Tobolsky model. The last exponent (**Fig. 8a**), determined first, contributes little to the total displacement. Apparently, it represents late-time diffusion and is expected to be a marginal contributor for Berea core. The second exponent (**Fig. 8b**) makes the dominant contribution and probably describes the main phenomena of desaturation by capillary drainage. The first exponent (**Fig. 8c**) makes a small, rapid contribution that corresponds with hydrodynamic penetration.

The description of the analysis for a reservoir sample, for example, is illustrated in **Fig. 9** using Sample #2 at a capillary pressure of 150 psi. Unlike for the Berea core, the last exponent (**Fig. 9a**) represents extended diffusion. The second exponent (**Fig. 9b**) reflects the small contribution of capillary drainage, and the first exponent (**Fig. 9c**), hydrodynamic displacement, acts very briefly. Analyses at other capillary pressures were similar, although most required only two exponential terms (**Table 4**).

RESISTIVITY MODELING

Parallel conductance models have been at the foundation of electrical resistivity modeling for interbedded shaley sands for many decades.[5-8] These, and other earlier modeling approaches, did not consider localized CT saturation measurements. The approach described here incorporates such measurements in a mathematical model for directly determining saturations within the sandy regions. Here we make the assumption that the sandy regions of the core behave in a similar manner during desaturation.

Considering a laminated shaley-sandstone core, the total resistivity R_t may be expressed as the sum of contributions from the shale and sandstone layers. Expressed mathematically:[2]

$$\frac{1}{R_t} = \frac{(1-a)}{R_{sh}} + \frac{a}{R_{ss}} \quad (4)$$

where a is the sand fraction, and R_{sh} and R_{ss} are the resistivities of the shale and sand, respectively. The total resistivity may be generalized using an arbitrary "power-law" expression:

$$R_t^w = (1-a)R_{sh}^w + a\ R_{ss}^w \tag{5}$$

where w represents a fitting parameter. According to Archie's Law, the resistivity of the sandy portion of the core may be expressed as:

$$R_{ss} = \frac{R_w}{f_{ss}^{m_{ss}} S_{w_{ss}}^{n_{ss}}} \tag{6}$$

where R_w is resistivity of the water, S_w is water saturation, and f is porosity. The symbols *m* and *n* represent formation factor and resistivity index, respectively, while the subscript *ss* represents quantities referring to the sandstone portions of a core. Substituting Eq. 6 into Eq. 5 yields the following:

$$R_t^w = (1-a)R_{sh}^w + a\ [\frac{R_w}{f_{ss}^{m_{ss}} S_{w_{ss}}^{n_{ss}}}]^w \tag{7}$$

For a completely saturated core (S_w = 1), and assuming $R_{sh} \approx R_{sh_o}$, Eq. 7 becomes:

$$R_o^w = (1-a)R_{sh_o}^w + a\ [\frac{R_w}{f_{ss}^{m_{ss}}}]^w \tag{8}$$

Subtracting Eq. 8 from Eq. 7 and collecting terms:

$$R_t^w - R_o^w = a\ (\frac{R_w}{f_{ss}^{m_{ss}}})^w [S_{w_{ss}}^{-w n_{ss}} - 1] \tag{9}$$

And defining $K = \frac{a\ R_w^w}{f_{ss}^{m_{ss} w}}$, and $n'_{ss} = w\ n_{ss}$ yields:

$$R_t^w - R_o^w = K\ [S_{w_{ss}}^{-n'_{ss}} - 1] \tag{10}$$

Eq. 10 is an expression for the difference between the measured resistivity of a core completely saturated with brine (R_o), and its resistivity at a particular stage of desaturation (R_t). This expression can be rewritten in terms of the water saturation in the sandy region of the core; indicating calculated water saturation as $S'_{w_{ss}}$:

$$S'_{w_{ss}} = [1 + \frac{R_t^w - R_o^w}{K}]^{-1/n'_{ss}} \tag{11}$$

In practice, the objective is to determine fitting parameters w and *K* to minimize the differences between measured and calculated water saturations. The criterion becomes:

$$e\ (w, K) = \sum\ \left(S'_{w_{ss}} - S_{w_{ss}}\right)^2 \tag{12}$$

where e is a minimized value. The procedure used here was to simultaneously iterate on the parameters *K* and n'_{ss} (w is calculated from its definition as n'_{ss} / n_{ss}).

Resistivity Modeling Results. The fitting parameter approach was applied to the experimental data sets for the reservoir samples. For simplicity, saturations for a sandstone region in the center slice of a core were modeled (i.e., saturation gradients neglected), and n_{ss} was taken as 2. **Fig. 10** shows a cross-plot of the calculated and measured saturations obtained by optimizing the parameters for each core. The fitting parameter *K* was determined at -0.39 for both samples, while n'_{ss} was determined as 0.120 and 0.070 for

Samples #1 and #2, respectively; corresponding e were 0.0095 and 0.0055. In the cross-plot, *K* was found to determine the slope of the relationship, while n'_{ss} established the vertical position in the x-y plane. The absolute discrepancies between calculated and measured saturations ranged from 2 to 4 saturation units.

The fitting parameters appear to lack physical significance, particularly in view of the negatively-signed *K*. This is not disallowed, however, by the approach which is based upon a general formulation (Eq. 5) that takes the resistivities to an arbitrary power. The procedure appears viable for practical application, provided small-scale saturation measurements (i. e., CT data) are made on reservoir core samples.

SUMMARY AND CONCLUSIONS

CT saturation monitoring of the interbedded cores showed preferential displacement of brine from high-permeability sands, and confirmed saturation gradients even at apparently stabilized test conditions.

Tobolsk's Technique is presented as a mathematical technique to represent capillary desaturation. Application to the experimental data successfully modeled the desaturation tests as a sequence of processes apparently dominated by different mechanisms.

A theoretical model is presented to utilize CT saturation measurements in a resistivity model. Used here, the model successfully represented saturations within sandy regions of interbedded cores. The technique has an advantage in that it requires only two fitting parameters and provides saturations specifically within the sandstone regions.

ACKNOWLEDGMENTS

The authors thank Unocal Corporation, Western Atlas, and the Azerbaijan State Oil Academy for permission to publish this work. For his help in the development of the resistivity model, we acknowledge Dr. Peter Day.

REFERENCES

1. Sprunt, E. S., Desal, K. P., Coles, M. E., Davis, R. M. and Muegge, E. L., "CT-Scan-Monitored Electrical-Resistivity Measurements Show Problems Achieving Homogeneous Saturation," *SPE Formation Evaluation* (June 1991) p. 134 - 140.
2. Day, P. I., personal communication.
3. Rutman, A. and Fligelman, H., "Formation Evaluation by Multidimensional Petrophysical Correlations in Azerbaijan," Soc. Core Analysts, Paper 9203 (1992).
4. Zemanek, J., "Low Resistivity hydrocarbon-Bearing Sand Reservoirs," *SPE Formation Evaluation* (Dec.1989) p. 515 - 521.
5. Waxman, M. H. and Smits, L. J. M., "Electrical Conductivities in Oil-Bearing Shaley Sands," *Soc. Pet. Eng. J.* (June 1968) p. 107 - 122.
6. Givens, W. W. and Schmidt, E. J., "A Generic Electrical Conduction Model for Low-Contrast Resistivity Sandstones," SPWLA 29th Annual Logging Symposium (June 1988) Paper E.
7. Herrick, D. C., "Conductivity Models, Pore Geometry, and Conduction Mechanisms," Paper D, Soc. Prof. Well Log Analysts 29th Annual Logging Symp. (June 1988).
8. Givens, W. W., "Formation Factor, Resistivity Index, and Related equations Based on a Conductive Rock Matrix Model (CRMM)," SPWLA 27th Annual Logging Symposium (June 1986) Paper P.
9. Tobolsky, A. V., *Properties and Structure of Polymers*, Khimiya, Moscow (1964).

TABLE 1 - PROPERTIES OF RESERVOIR CORE PLUGS

DEPTH, FT:	13116.7	13140.8
Length, cm:	4.88	4.74
Area, sq-cm:	11.4	11.4
Porosity, %:	24.22	17.23
Permeability, mD:	1.02	0.31
Clay Content, %:	40	30

TABLE 2 - CT RESISTIVITY TESTS OF RESERVOIR SAMPLES

Capillary Press. (psi)	Ave. Water Saturation (Fract.)	Sand Water Saturation (Fract.)	Resistance (ohms)	Resistivity (ohm-m)	Resistivity Index
Plug 13116.7 ft.:					
0.0	1.000	1.00	473	11.05	-
5.0	0.958	0.886	492	11.49	1.040
10.0	0.706	0.612	602	14.06	1.273
19.5	0.654	0.557	644	15.04	1.361
60.	0.570	0.493	686	16.03	1.449
100.	0.516	0.433	724	16.91	1.529
150.	0.405	0.368	751	17.54	1.587
Plug 13140.8 ft.:					
0.0	1.000	1.00	527	12.67	-
5.0	0.924	0.876	591	14.21	1.120
15.	0.768	0.687	699	16.81	1.325
30	0.697	0.558	764	18.37	1.448
60.	0.608	0.464	830	19.96	1.575
150.	0.518	0.400	907	21.81	1.721

TABLE 3 - RESULTS OF EVOLUTIONAL MODELING

TEST	PRES. (psi)	TIME STEP (min)	DURATION (min)	MODEL PARAMETERS A	B	α	TIME (min)
Berea,	5	1 -.13	12	-40.213	40.214	0.0019	
EX 600		14-25	11	108.82	-108.514	-0.0005	
		26-56	30	7.54	-7.564	-0.01	
		57-382	325	20.261	-19.784	-0.0027	
		644		14.074	-1.43	-0.0017	4000
13116.7 ft	5	0-300	300	0.51	-0.348	-0.034	
Doped MO		406-1787	1381	0.24	-0.216	-0.0008	
		>2119(4580)	2461	0.325	-0.241	-0.0004	22500
	10	1-308	307	1.045	-0.814	-0.0016	
		368-2348	1980	1.807	-1.647	-0.0009	
		>2517(4059)	1542	1.841	-0.886	-0.0005	17000
	20	1-340	339	1.851	-0.122	-0.0065	
		580-1615	1035	2.058	-0.295	-0.0008	
		>1975(5157)	3182	2.216	-0.432	-0.0003	25000
	60	2-345	343	2.236	-0.106	-0.0224	
		366-1746	1380	2.545	-0.336	-0.0005	
		>2106(4605)	2499	2.842	-0.559	-0.0001	75000
	100	3-942	939	2.69	-0.137	-0.0012	
		>1341(5214)	3873	2.885	-0.317	-0.0003	23500
	150	1-225	224	2.823	-0.037	-0.112	
		422-1725	1303	2.972	-0.144	-0.0004	
		>3226(5566)	2340	2.949	-0.079	-0.0003	185000
13140.8 ft	5	0-90	90	0.096	-0.089	-0.0204	
Doped MO		150-6665	6512	0.487	-0.407	-0.0004	
		>6722		0.733	-0.551	-0.0001	89000
	15	0-30	30	0.205	0.347	-0.0049	
		31-1662	1631	1.524	-0.993	-0.0023	
		>1722		1.971	-0.721	-0.0003	27500
	30	0-72	72	1.81	-0.031	-0.0549	
		77-1218	1141	2.084	-0.287	-0.0007	
		>1278		2.966	-1.094	-0.0001	82000
	60	0-2	2	2.323	0.007	0.258	
		3-.46	43	2.355	-0.021	-0.0341	
		106-1486	1380	2.638	-0.0294	-0.0006	
		>1546		3.094	-0.721	-0.0002	39000
	150	0-9	9	2.717	0.131	0.0125	
		10-.97	87	2.913	-0.056	-0.0144	
		112-1935	1823	3.186	-0.307	-0.0007	
		>1995		3.273	-0.36	-0.0004	175000

TABLE 4 - RESULTS OF TOBOLSKY TECHNIQUE

TEST	PRES. (psi)	TIME STEP (min.)	MODEL PARAMETERS	
			A	α
Berea, EX600	5	>644	1.304	-0.00161
		25-119	12.58	-0.00479
		0-5	0.219	-0.20288
13116.7 ft Doped MO	5	>3499	0.245	-0.00037
		0-406	0.082	-0.00248
	10	>5217	0.897	-0.00051
		0-45	0.717	-0.00161
	20	>3213	0.446	-0.00031
		0-100	0.02	-0.0302
	60	>2586	0.561	-0.00015
		0-90	0.128	-0.00508
	100	>4261	0.131	-0.00014
		0-321	0.192	-0.00066
	150	>3226	0.079	-0.0003
		0-225	0.073	-0.00241
13140.8 ft Doped MO	5	>6242	0.545	-0.00011
		0-60	0.179	-0.00679
	15	>1148	0.732	-0.00029
		0-91	0.689	-0.00258
	30	>1498	1.092	-0.00008
		0-16	0.09	-0.00837
	60	>405	0.724	-0.00016
		36-346	0.029	-0.00359
		0-4	0.012	-0.2292
	150	>893	0.363	-0.00043
		77-413	0.037	-0.00406
		0-9	0.027	-0.09522

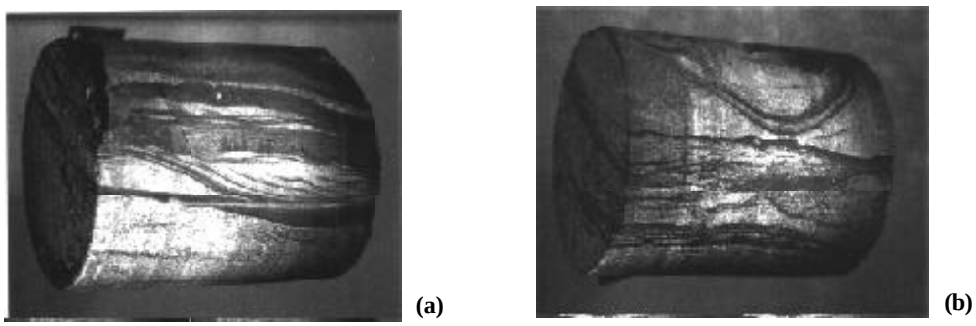

Fig. 1 - Photographs of reservoir core samples: (a) Sample #1 (13,116.7 ft), and (b) Sample #2 (13,140.8 ft).

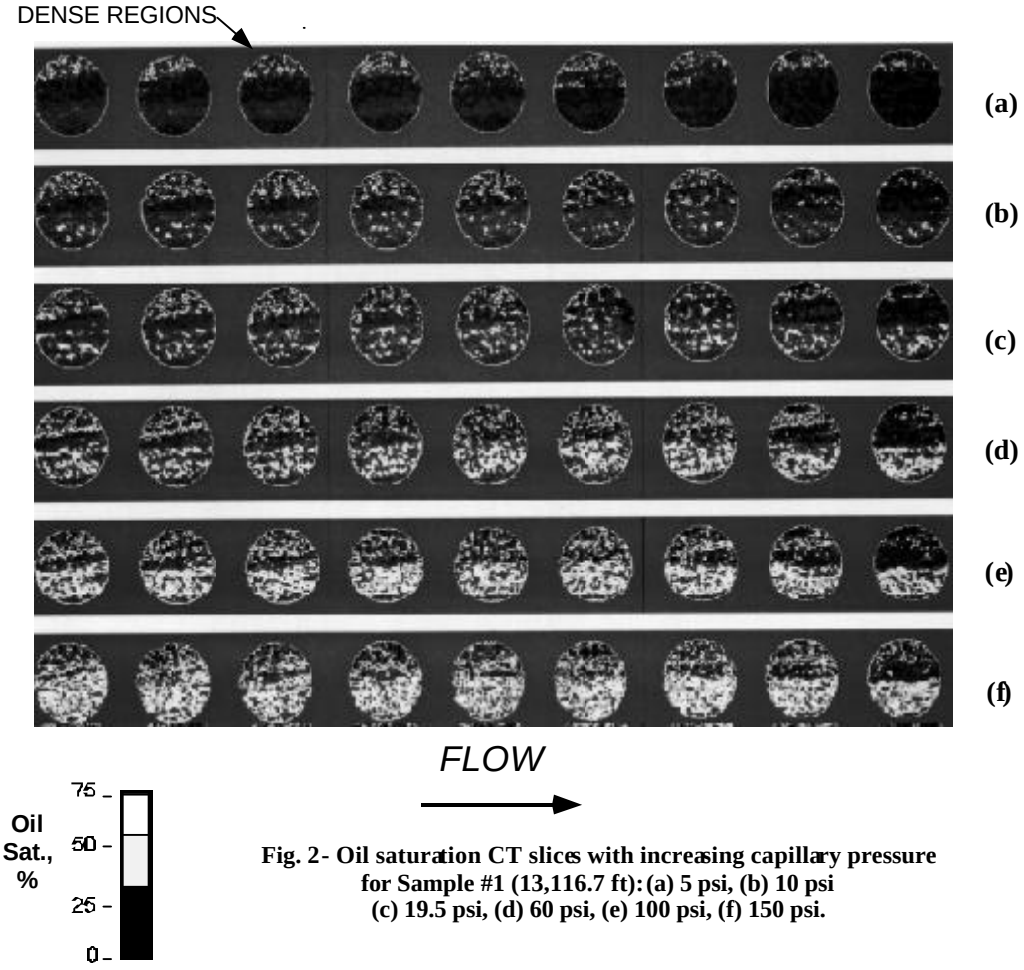

Fig. 2 - Oil saturation CT slices with increasing capillary pressure for Sample #1 (13,116.7 ft): (a) 5 psi, (b) 10 psi (c) 19.5 psi, (d) 60 psi, (e) 100 psi, (f) 150 psi.

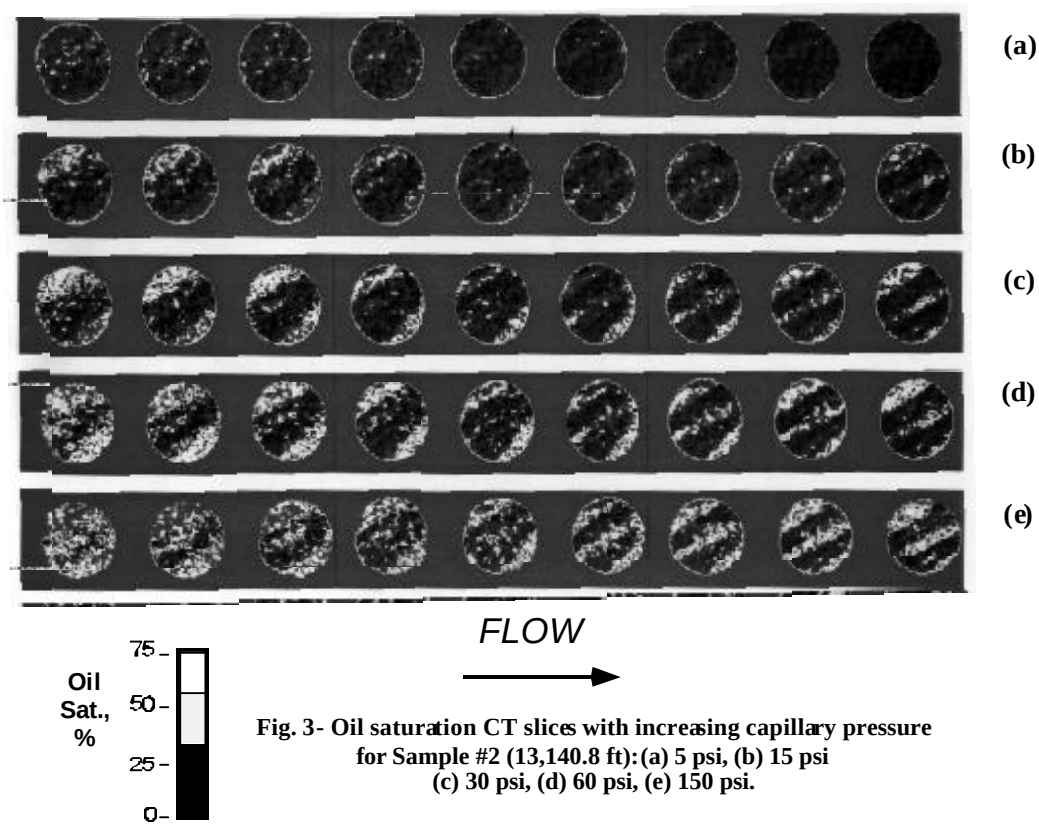

Fig. 3- Oil saturation CT slices with increasing capillary pressure for Sample #2 (13,140.8 ft): (a) 5 psi, (b) 15 psi (c) 30 psi, (d) 60 psi, (e) 150 psi.

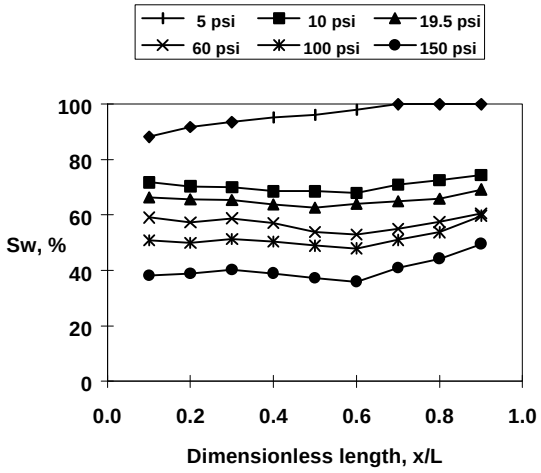

Fig. 4 - Water saturations during displacement test, Sample #1 (13,116.7 ft).

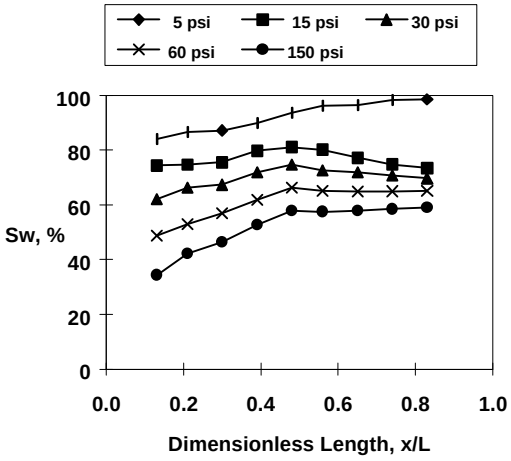

Fig. 5 - Water saturations during displacement test, Sample #2 (13,140.8 ft).

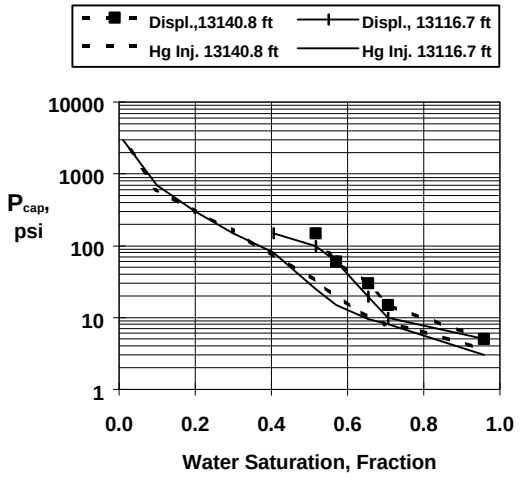

Fig. 6 - Capillary pressures from displacements and mercury injection tests.

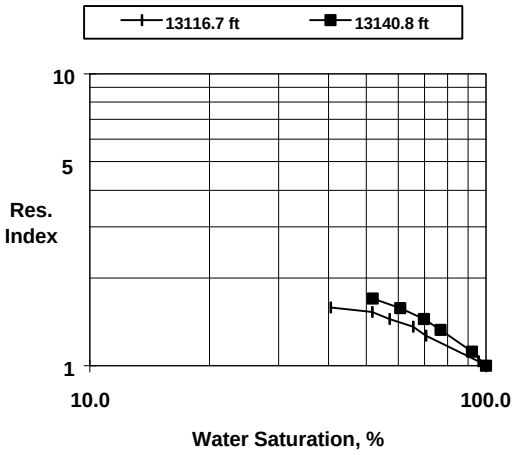

Fig. 7 - Resistivity results from displacement tests.

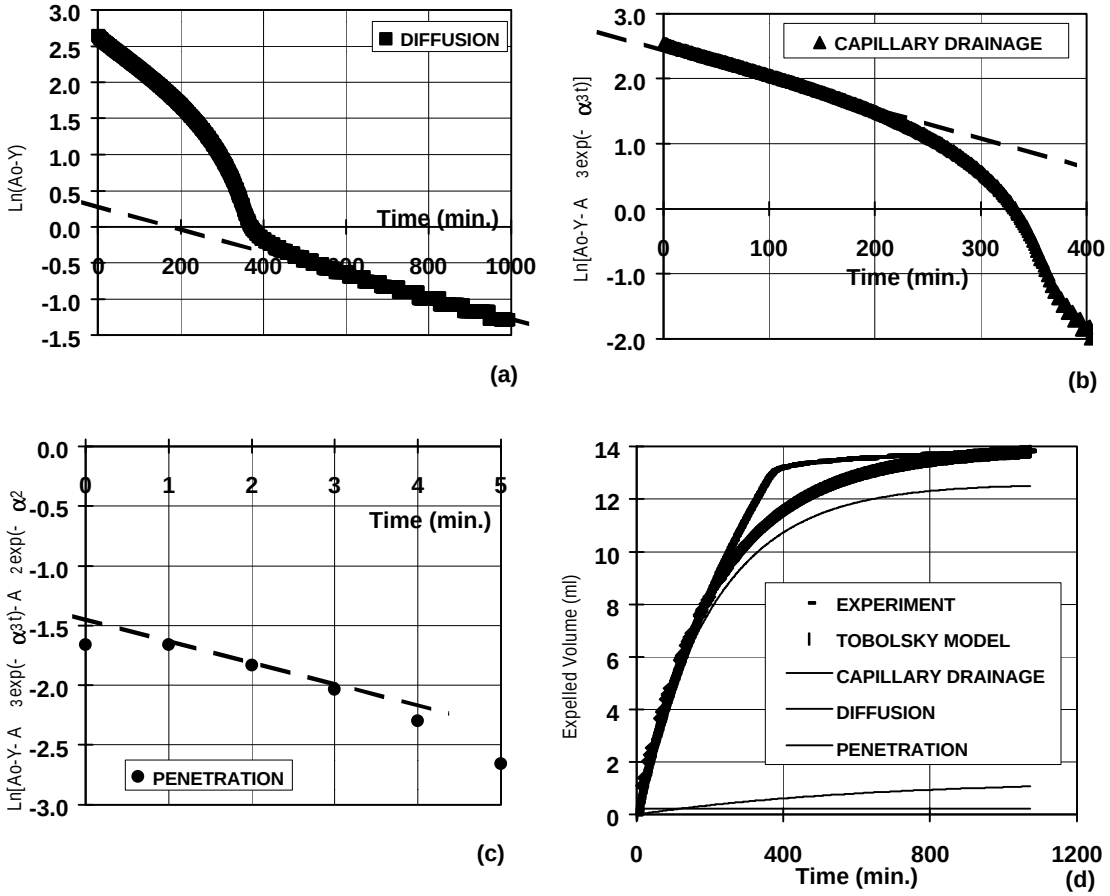

Fig. 8 - Application of Tobolsky Technique to model capillary displacement for Berea core: (a) late time diffusion, (b) capillary displacement, (c) initial penetration, and (d) Tobolsky model, experimental data, and influence of individual terms.

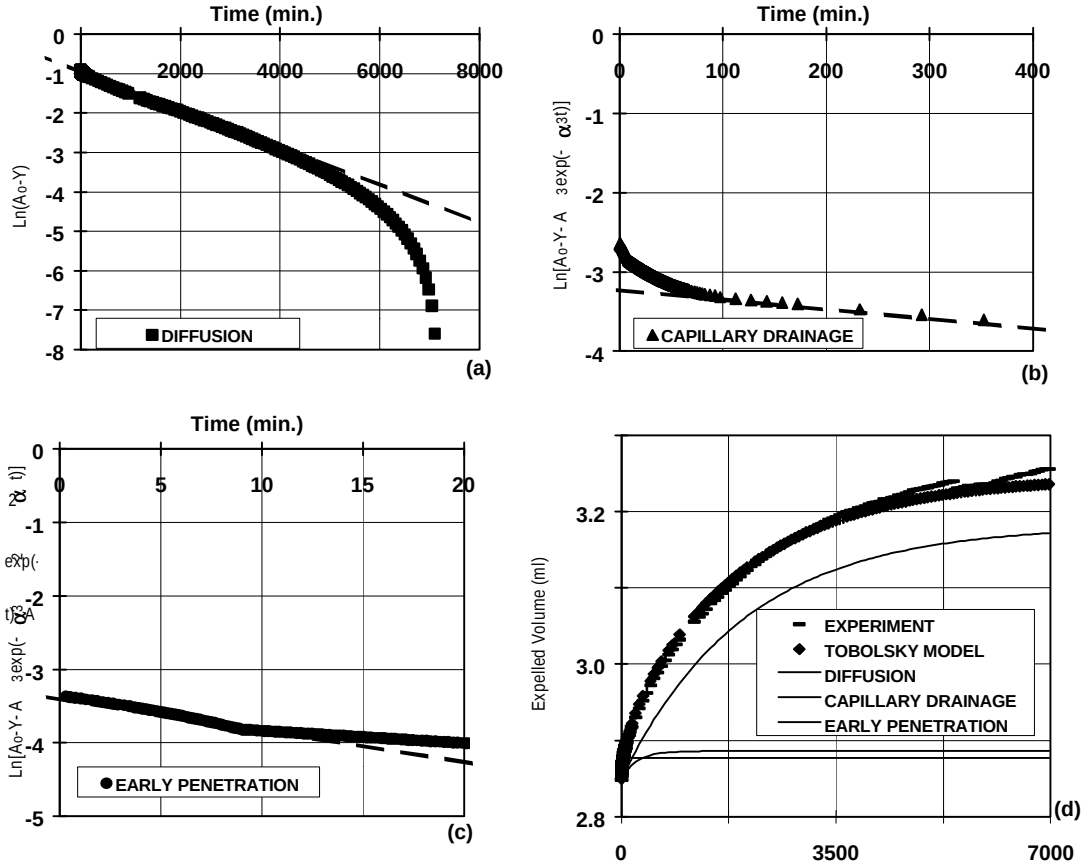

Fig. 9 - Application of Tobolsky Technique to model capillary displacement: Sample 2 (13,140.8 ft), at 150 psi: (a) capillary displacement, (b) late penetration, (c) early penetration, and (d) the Tobolsky model, experimental data, and influence of individual terms.

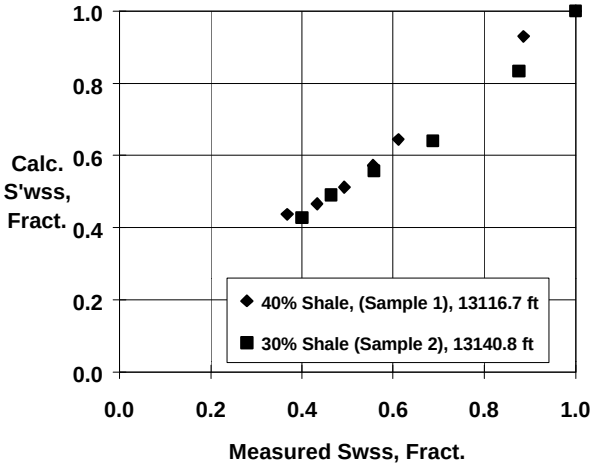

Fig. 10 - Comparison of calculated and measured water saturations in sandstone regions of the cores.